

Gas-Phase Electron Transfer Reactions from Multiply-Charged Anions to Rare Gas Cations[†]

William J. Herron, Douglas E. Goeringer, and Scott A. McLuckey*

Contribution from the Chemical and Analytical Sciences Division, Oak Ridge National Laboratory, Oak Ridge, Tennessee 37831-6365

Received June 21, 1995[⊗]

Abstract: Multiply-charged anions derived from electrospray have been subjected to reactions with singly-charged cations of argon, krypton, and xenon in a quadrupole ion trap. The doubly-charged anion formed from a sulfonated azo dye and the highest negative charge states formed from the polyadenylates 5'-d(AAA)-3', 5'-d(AAAA)-3', and 5'-d(AAAAA)-3' served as the anionic reactants. In each case, extensive fragmentation of the anionic product, which presumably is a radical anion, was observed. Comparison of the observed decomposition products arising from ion/ion reactions with product anions formed via collisional activation of the even-electron species of the same charge state, as formed directly by electrospray, shows significant differences. While both the even-electron and odd-electron species hold some fragmentation pathways in common, the odd-electron species show one or more additional decomposition channels. Furthermore, in the case of the polyadenylate anions, the ion/ion reactions showed more nearly equal contributions from the major dissociation channels that yield sequence information than did collisional activation of the corresponding even-electron anions.

Introduction

Gas-phase multiply-charged ions derived from large polyatomic molecules, including biopolymers, have recently become amenable to study due to the advent of electrospray,¹ matrix assisted laser desorption,² and massive cluster impact.³ These species present new challenges to the ion chemist due to their large numbers of degrees of freedom and to the unique condition in which like charges are present on the molecule at remote locations. Both the multiplicity of possible higher order structures and the influence of internal Coulombic repulsion add to the complexity in understanding the behavior of these ions in the gas phase. Nevertheless, the rapidly growing importance of the ionization methods just mentioned, most notably in biochemical research, makes issues of multiply-charged ion structure and reactivity particularly relevant.

While multiple charging adds a new dimension of complexity in understanding ion chemistry, it can facilitate the study of

high mass ions by reducing mass-to-charge ratios, and by increasing the likelihood that reaction products carry charge. The latter characteristic facilitates the study of multi-step reaction sequences via one or more of a variety of tools available to the ion chemist. Ion chemistry studies to date have principally emphasized unimolecular reactions involving dissociation.⁴ Such reactions have typically involved some form of ion activation,

[†] Research was supported by the National Institutes of Health under Grant No. GM45372. Oak Ridge National Laboratory is managed for the United States Department of Energy by Lockheed Martin Energy Systems, Inc. under Contract No. DE-AC05-84OR21400.

[⊗] Abstract published in *Advance ACS Abstracts*, November 1, 1995.

(1) (a) Yamashita, M.; Fenn, J. B. *J. Phys. Chem.* **1984**, *88*, 4451–4459. (b) Yamashita, M.; Fenn, J. B. *J. Phys. Chem.* **1984**, *88*, 4671–4675. (c) Aleksandrov, M. L.; Gall, L. N.; Krasnov, N. V.; Nikolaev, V. I.; Paulenko, V. A.; Shkurov, V. A. *Dokl. Phys. Chem. (Engl.)* **1984**, *277*, 572–575. (d) Wong, S. F.; Meng, C. K.; Fenn, J. B. *J. Phys. Chem.* **1988**, *92*, 546–550. (e) Meng, C. K.; Mann, M.; Fenn, J. B. *Z. Phys. D: At. Mol. Clusters* **1988**, *10*, 361–368. (f) Fenn, J. B.; Mann, M.; Meng, C. K.; Wong, S. F.; Whitehouse, C. M. *Science* **1990**, *246*, 64–71. (g) Smith, R. D.; Loo, J. A.; Edmonds, C. G.; Barinaga, C. J.; Udseth, H. R. *Anal. Chem.* **1990**, *62*, 882–899. (h) Fenn, J. B.; Mann, M.; Meng, C. K.; Wong, S. F.; Whitehouse, C. M. *Mass Spectrom. Rev.* **1990**, *9*, 37–70. (i) Smith, R. D.; Loo, J. A.; Ogorzalek Loo, R. R.; Busman, M.; Udseth, H. R. *Mass Spectrom. Rev.* **1991**, *10*, 359–451. (j) Mann, M. *Org. Mass Spectrom.* **1990**, *25*, 575–587. (k) Huang, E. C.; Wachs, T.; Conboy, J. J.; Henion, J. D. *Anal. Chem.* **1990**, *62*, 713A–725A. (2) (a) Karas, M.; Hillenkamp, F. *Anal. Chem.* **1988**, *60*, 2299–2301. (b) Overberg, A.; Karas, M.; Hillenkamp, F. *Rapid Commun. Mass Spectrom.* **1991**, *5*, 128–131. (c) Nordhoff, E.; Ingedoh, A.; Cramer, R.; Overberg, A.; Stahl, B.; Karas, M.; Hillenkamp, F.; Crain, P. F. *Rapid Commun. Mass Spectrom.* **1992**, *6*, 771–776. (3) (a) Mahoney, J. F.; Perel, J.; Ruatta, S. A.; Martino, P. A.; Husain, S.; Lee, T. D. *Rapid Commun. Mass Spectrom.* **1991**, *5*, 441–445. (b) Mahoney, J. F.; Perel, J.; Lee, T. D.; Martino, P. A.; Williams, P. J. *Am. Soc. Mass Spectrom.* **1992**, *3*, 311–317.

(4) (a) Barinaga, C. J.; Edmonds, C. G.; Udseth, H. R.; Smith, R. D. *Rapid Commun. Mass Spectrom.* **1989**, *3*, 160–164. (b) Smith, R. D.; Barinaga, C. J.; Udseth, H. R. *J. Phys. Chem.* **1989**, *93*, 5019–5022. (c) Smith, R. D.; Loo, J. A.; Barinaga, C. J.; Edmonds, C. G.; Udseth, H. R. *J. Am. Soc. Mass Spectrom.* **1990**, *1*, 53–65. (d) Loo, J. A.; Edmonds, C. G.; Smith, R. D. *Anal. Chem.* **1991**, *63*, 2488–2499. (e) Rockwood, A. L.; Busman, M.; Smith, R. D. *Int. J. Mass Spectrom. Ion Processes* **1991**, *111*, 103–129. (f) Busman, M.; Rockwood, A. L.; Smith, R. D. *J. Phys. Chem.* **1992**, *96*, 2397–2400. (g) Loo, J. A.; Quinn, J. P.; Ryu, S. I.; Henry, K. D.; Senko, M. W.; McLafferty, F. W. *Proc. Natl. Acad. Sci. U.S.A.* **1992**, *89*, 286–289. (h) Loo, J. A.; Edmonds, C. G.; Smith, R. D. *Anal. Chem.* **1993**, *65*, 425–438. (i) Feng, R.; Konishi, Y. *Anal. Chem.* **1993**, *65*, 645–649. (j) Senko, M. W.; Beu, S. C.; McLafferty, F. W. *Anal. Chem.* **1994**, *66*, 415–417. (k) Senko, M. W.; Speir, J. P.; McLafferty, F. W. *Anal. Chem.* **1994**, *66*, 2801–2808. (l) Little, D. P.; Speir, J. P.; Senko, M. W.; McLafferty, F. W. *Anal. Chem.* **1994**, *66*, 2809–2815. (m) Fabris, D.; Kelly, M.; Wu, Z.; Fenselau, C. *Rapid Commun. Mass Spectrom.* **1994**, *8*, 791–795.

(5) (a) McLuckey, S. A.; Van Berkel, G. J.; Glish, G. L. *J. Am. Chem. Soc.* **1990**, *112*, 5668–5670. (b) McLuckey, S. A.; Glish, G. L.; Van Berkel, G. J. *Anal. Chem.* **1991**, *63*, 1971–1978. (c) Ogorzalek Loo, R. R.; Udseth, H. R.; Smith, R. D. *J. Phys. Chem.* **1991**, *95*, 6412–6415. (d) McLuckey, S. A.; Glish, G. L.; Van Berkel, G. J. Proceedings of the 39th ASMS Conference on Mass Spectrometry and Allied Topics; Nashville, TN, 1991; pp 901–902. (e) Bursey, M. M.; Pedersen, L. G. *Org. Mass Spectrom.* **1992**, *27*, 974–975. (f) Winger, B. E.; Light-Wahl, K. J.; Smith, R. D. *J. Am. Soc. Mass Spectrom.* **1992**, *3*, 624–630. (g) Ogorzalek Loo, R. R.; Loo, J. A.; Udseth, H. R.; Fulton, J. L.; Smith, R. D. *Rapid Commun. Mass Spectrom.* **1992**, *6*, 159–165. (h) Ikononou, M. G.; Kebarle, P. *Int. J. Mass Spectrom. Ion Proc.* **1992**, *117*, 283–298. (i) Winger, B. E.; Light-Wahl, K. J.; Rockwood, A. L.; Smith, R. D. *J. Am. Chem. Soc.* **1992**, *114*, 5897–5898. (j) Cassady, C. J.; Wronka, J.; Kruppa, G. H.; Laukien, F. H. *Rapid Commun. Mass Spectrom.* **1994**, *8*, 394–400. (k) Ogorzalek Loo, R. R.; Smith, R. D. *J. Am. Soc. Mass Spectrom.* **1994**, *5*, 207–220. (l) Hunter, A. P.; Severs, J. C.; Harris, F. M.; Games, D. E. *Rapid Commun. Mass Spectrom.* **1994**, *8*, 417–422. (m) Ogorzalek-Loo, R. R.; Winger, B. E.; Smith, R. D. *J. Am. Soc. Mass Spectrom.* **1994**, *5*, 1064–1071. (n) McLuckey, S. A.; Goeringer, D. E. *Anal. Chem.* **1995**, *67*, 2493–2497. (o) McLuckey, S. A.; Van Berkel, G. J.; Glish, G. L.; Schwartz, J. C. In *Modern Mass Spectrometry: Practical Aspects of Ion Trap Mass Spectrometry*, March, R. E., Todd, J. F. J., Eds.; CRC Press: Boca Raton, 1995; Vol. 2, Chapter 3.

most frequently via energetic collisions. Several groups have also studied ion/molecule reactions involving proton transfers between a multiply-charged ion and a neutral acid or base.⁵ McLafferty et al. have studied H/D exchange reactions by use of gaseous D₂O the results from which suggest that distinct higher order structures of multiply-protonated proteins can co-exist in the dilute gas phase depending upon the method of ion preparation.⁶

While most ion chemistry studies involving multiply-charged ions have involved inelastic and reactive collisions with neutral atoms and molecules, a few reports have also appeared involving ion/ion reactions. Ogorzalek-Loo et al., for example, have reported on the merging of oppositely charged ions in a high-pressure region within an electrospray ion source.⁷ Recently, we reported on the proton transfer reactions of oppositely charged ions within the context of a tandem mass spectrometry experiment in a Paul trap.⁸ These studies involved the protonation of multiply-charged oligonucleotide anions by protonated pyridine. We noted that essentially no fragmentation was observed in these reactions despite the rather large exothermicity expected for mutual neutralization. It was inferred from these observations that the relative translation created by the attraction of oppositely-charged ions is apparently not partitioned efficiently into internal degrees of freedom of the products upon proton transfer.

In this paper, we describe the study by tandem mass spectrometry of gas-phase electron transfer reactions involving multiply-charged closed shell anions and the rare gas cations of argon, krypton, and xenon. This constitutes an ion/ion reaction type for which an ion/molecule reaction analog involving a multiply-charged biopolymer has yet to be demonstrated. That is, while proton transfer ion/molecule reactions were noted long before ion/ion proton transfer was studied, there is no evidence as yet for electron transfer in the gas phase involving a high-mass multiply-charged even-electron biomolecule.⁹ In the case of multiply-charged closed shell anions reacting with rare gas cations, the initially formed charged product is assumed to be a radical anion. Odd-electron multiply-charged ions are not formed directly by any of the ionization methods that yield multiply-charged high mass ions. The ability to form such ions in the gas phase by ion/ion electron transfer, therefore, might provide information complementary to that available from closed-shell ions.

Experimental Section

Samples and Apparatus. The oligonucleotides 5'-d(AAA)-3', 5'-d(AAAA)-3', and 5'-d(AAAAA)-3' were obtained from Pharmacia, Milwaukee, WI, as the sodium salts. The dye Direct Red 81 was obtained from Aldrich, St. Louis, MO. Solutions were prepared by dissolving the sample in a drop of HPLC-grade water and diluting with HPLC-grade methanol to give a concentration of 1–25 μ M in at least 9:1 methanol–water (v/v). All solutions were infused at rates of 0.25–1.0 μ L/min through a 120 μ m i.d. needle held at a potential of –3000 to –3500 V.

(6) Suckau, D.; Shi, Y.; Beu, S. C.; Senko, M. W.; Quinn, J. P.; Wampler, F. M., III; McLafferty, F. W. *Proc. Natl. Acad. Sci. U.S.A.* **1993**, *90*, 790–793.

(7) (a) Ogorzalek-Loo, R. R.; Udseth, H. R.; Smith, R. D. *J. Phys. Chem.* **1991**, *95*, 6412–6415. (b) Ogorzalek Loo, R. R.; Udseth, H. R.; Smith, R. D. *J. Am. Soc. Mass Spectrom.* **1992**, *3*, 695–705.

(8) Herron, W. J.; Goeringer, D. E.; McLuckey, S. A. *J. Am. Soc. Mass Spectrom.* **1995**, *6*, 529–532.

(9) Several groups have reported results regarding electron transfer involving multiply-charged ions of buckminsterfullerene, and derivatives thereof, and neutral molecules in the gas phase. See, for example: (a) McElvany, S. W.; Ross, M. M.; Callahan, J. H. *Mater. Res. Soc. Symp. Proc.* **1991**, *206*, 697–701. (b) Petrie, S.; Javahery, G.; Wang, J.; Bohme, D. K. *J. Phys. Chem.* **1992**, *96*, 6121–6123. (c) Stry, J. J.; Coolbaugh, M. T.; Turos, E.; Garvey, J. F. *J. Am. Chem. Soc.* **1992**, *114*, 7914–7916. (d) Jin, C.; Hettich, R. L.; Compton, R. N.; Tuinman, A.; Derecskei-Kovacs, A.; Marynick, D. S.; Dunlap, B. I. *Phys. Rev. Lett.* **1994**, *73*, 2821–2824.

All experiments were carried out with a home-made electrospray source coupled with a Finnigan-MAT (San Jose, CA) ion trap mass spectrometer modified for injection of ions formed external to the ion trap. Details of the electrospray/ion trap interface have been described.¹⁰ Electron ionization was effected by drilling a 3 mm diameter hole through the ring electrode and by mounting a heated filament near the ring electrode such that electrons could be gated into the trapping volume. The electron gate electrode was controlled by a variable length pulse generator (Stanford Research Systems, Model 535) actuated by a trigger pulse from the ion trap mass spectrometer electronics. This arrangement allowed for independent control of anion accumulation and cation formation. In all cases, the multiply-charged parent anions were accumulated and isolated prior to cation formation.

For the case of ion/molecule proton transfer involving dianions of Direct Red 81, trifluoroacetic acid served as the gaseous acid and was admitted into the vacuum system to a pressure of roughly 1×10^{-7} Torr. For the case of ion/ion proton transfer involving dianions of Direct Red 81, protonated pyridine served as the cationic reagent. Pyridine vapor was leaked into the vacuum chamber to a pressure of $1-3 \times 10^{-7}$ Torr. At this pressure, the radical cation of pyridine is converted quantitatively to protonated pyridine via self-chemical ionization within 10 ms. This time frame is short relative to the reaction times of several hundred milliseconds to one second required for significant formation of ion/ion reaction products. For the ion/ion electron transfer experiments, one of the ionized rare gases (argon, krypton, or xenon) served as the cationic reagent. The rare gas was admitted to a pressure of $\sim 5 \times 10^{-6}$ Torr (uncorrected) and the duration of the ionizing electron pulse was adjusted to accumulate a sufficient number of cations to yield product ions over the course of several hundred milliseconds of anion/cation storage. Argon, krypton and, to a lesser extent, xenon ions undergo charge exchange with low mass background species in the vacuum system requiring much longer ionization times (up to 30 ms) than required for the protonated reagent involved in the ion/ion proton transfer experiments.

Ion Manipulation and Mass/Charge Analysis. Anions were injected axially into the ion trap for periods ranging from 0.1 to 1.0 s. The radio-frequency (rf) sine-wave amplitude applied to the ring electrode during ion injection ranged from 700 to 1000 V zero-to-peak. In all cases, helium was admitted into the vacuum system to a total pressure of 1 mTorr with a background pressure in the instrument of 2×10^{-5} Torr without the addition of helium.

Details of ion isolation for high-mass multiply-charged ions have been given previously.¹¹ A single resonance ejection scan was used for isolation of parent ions. Low m/z ions were ejected by passing the ions through a q_z value of 0.908 by scanning the amplitude of the ring-electrode rf sine wave. High m/z ions were ejected by dipolar resonance ejection scan using a 12 V p-p sine-wave signal applied to the end caps at a frequency selected to eject ions at an m/z value slightly greater than that of the parent ion. Parent ions were isolated prior to the 0.2–1.0 s ion/ion reaction period at less than unit resolution to avoid parent ion loss, due either to dissociation or ejection from off-resonance power absorption.

Mass/charge analysis was effected after the completion of all ion isolation and reaction periods using resonance ejection¹² to yield a mass/charge range of 1300. The mass/charge scale for the ion/ion reaction spectra was calibrated using the electrospray mass spectrum of the parent compound. In this work, the mass/charge ratios of the various charge states of the parent compound were known and could be used to determine a correction for the mass scale provided by the ion trap data system. The mass accuracy associated with mass/charge assignments in the MS/MS and MSⁿ experiments is on the order of 0.2% or better. The spectra shown here were typically the result of an average of 50–100 individual scans.

(10) (a) Van Berkel, G. J.; McLuckey, S. A.; Glish, G. L. *Anal. Chem.* **1990**, *62*, 1284–1295. (b) McLuckey, S. A.; Van Berkel, G. J.; Glish, G. L.; Huang, E. C.; Henion, J. D. *Anal. Chem.* **1991**, *63*, 375–383.

(11) McLuckey, S. A.; Goeringer, D. E.; Glish, G. L. *J. Am. Soc. Mass Spectrom.* **1991**, *2*, 11–21.

(12) (a) Kaiser, R. E., Jr.; Cooks, R. G.; Moss, J.; Hemberger, P. H. *Rapid Commun. Mass Spectrom.* **1989**, *3*, 50–53. (b) Kaiser, R. E., Jr.; Louris, J. N.; Amy, J. W.; Cooks, R. G. *Rapid Commun. Mass Spectrom.* **1989**, *3*, 225–229.

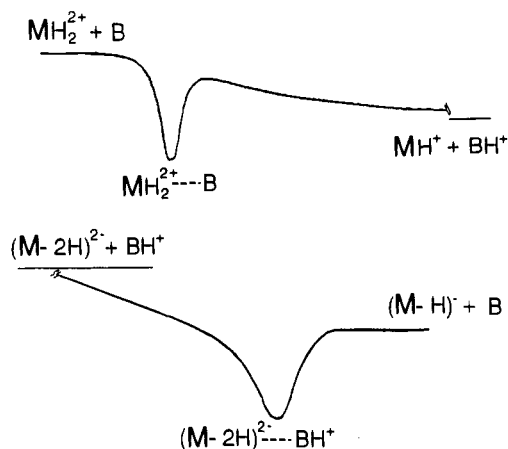
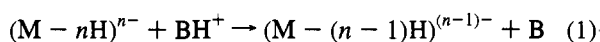


Figure 1. Energy diagrams for multiply-charged ion/molecule and multiply-charged ion/ion proton transfer reactions.

Results and Discussion

In comparing and contrasting ion/ion reactions with ion/molecule reactions it is important to recognize that the reactions proceed over very different energy surfaces. While proton transfer, for example, involving multiply-charged ions reacting both with neutrals and with oppositely charged ions has been demonstrated, the thermodynamics and the kinetics of the reactions are very different. Figure 1 shows generic energy diagrams for ion/molecule and ion/ion proton transfer reactions drawn in analogy with the Brauman diagram¹³ often used to represent proton transfer reactions. The entrance channel for the multiply-charged ion/molecule reaction is governed at long range by attractive polarization forces whereas the exit channel, in which two products of like charge are formed, is dominated by a repulsive $1/r$ potential at long range. This creates a barrier in the exit channel the magnitude of which is determined by the strength of the Coulomb field at the transition state. The occurrence or non-occurrence of the reaction is therefore not determined solely by the relative thermodynamic stabilities of the reactants and products. This situation has been discussed within the context of the chemistry of both small multiply-charged ions¹⁴ and high-mass multiply-charged ions.⁵ In contrast, the ion/ion reaction is dominated by the long-range attractive $1/r$ potential in the entrance channel and there is no Coulomb barrier in the exit channel. There are, therefore, two major consequences. First, multiply-charged ion/ion reaction rate constants are significantly greater than those of multiply-charged ion/molecule reactions.¹⁵ Second, ion/ion reactions are much more exothermic and exoergic than are multiply-charged ion/molecule reactions.

The thermodynamic quantities that determine the reaction enthalpy in the case of multiply-charged ion/ion proton transfer reactions of the form



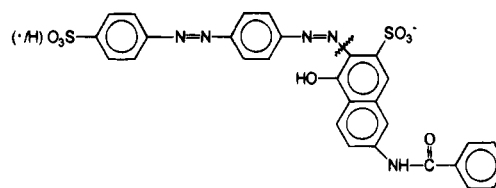
where M represents the neutral high-mass molecule and B represents a neutral base, are the proton affinity of B and the

(13) Jasinski, J. M.; Brauman, J. I. *J. Am. Chem. Soc.* **1980**, *102*, 2906–2913.

(14) (a) Tonkyn, R.; Weisshaar, J. C. *J. Am. Chem. Soc.* **1986**, *108*, 7128–7130. (b) Roth, L. M.; Freiser, B. S. *Mass Spectrom. Rev.* **1991**, *10*, 303–328. (c) Petrie, S.; Javahery, G.; Wincel, H.; Bohme, D. K. *J. Am. Chem. Soc.* **1993**, *115*, 6290–6294. (d) Javahery, G.; Petrie, S.; Wincel, H.; Wang, J.; Bohme, D. K. *J. Am. Chem. Soc.* **1993**, *115*, 6295–6301.

(15) We estimated the rate constant for triply-charged 5'-d(AAAA)-3' reacting with protonated pyridine to be on the order of 10^{-7} cm³/(molecule·s)⁸ whereas multiply-charged ion/molecule proton transfer reactions rate constants are generally less than 10^{-7} cm³/(molecule·s).^{5a,j}

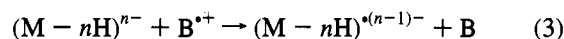
Chart 1



proton affinity of $(M - nH)^{n-}$ (or its equivalent, the gas-phase acidity of $(M - (n - 1)H)^{(n-1)-}$). That is:

$$\Delta H_{\text{rxn}} = \text{PA}(B) - \text{PA}(M - nH)^{n-} \quad (2)$$

Even singly-charged anions of the strongest acids will neutralize protonated molecules of the highest proton affinities. Multiple charging of the anion will tend to make the reactions even more exothermic. In the case of electron transfer reactions of the form



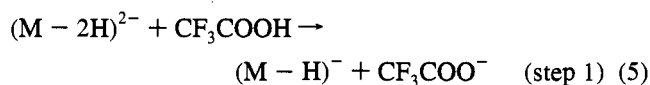
the thermodynamics are governed by the ionization potential of B and the electron affinity of $(M - nH)^{(n-1)-}$. That is,

$$\Delta H_{\text{rxn}} = \text{EA}((M - nH)^{(n-1)-}) - \text{IP}(B) \quad (4)$$

This reaction is expected to be highly exothermic with virtually any combination of radical cation and multiply-charged anion, assuming the neutral of the radical cation to be formed in its ground electronic state.

Ion/ion electron and ion/ion proton transfer reactions differ from the point of view of reaction energetics, but perhaps equally important, the nature of the products differ. In the preceding generic example, the anionic product from proton transfer, $(M - (n - 1)H)^{(n-1)-}$, is an even-electron species that might be formed directly via electrospray whereas the anionic product from electron transfer, $(M - nH)^{(n-1)-}$, is an odd-electron species that might be difficult to form otherwise. The following data describe a number of experiments in which ion/ion electron transfer is emphasized. However, results from ion/molecule proton transfer and ion/ion proton transfer reactions are also either presented or described to highlight the phenomenology associated with the electron transfer reactions.

Direct Red 81. The sulfonated azo dye, Direct Red 81, shown in Chart 1, is observed predominantly as the dianion in the electrospray mass spectrum. Ion/molecule proton transfer from trifluoroacetic acid admitted into the ion trap vacuum system can be used to form the singly-deprotonated molecule and ion trap collisional activation can subsequently be used to induce fragmentation. Figure 2a shows the spectrum resulting from the sequence



Step 2 involves ion trap collisional activation of the $(M - H)^-$ ion. No fragmentation was associated with the ion/molecule proton transfer reaction itself (data not shown). The only products observed upon storage of the dianion in the presence of trifluoroacetic acid corresponded in mass-to-charge to $(M - H)^-$ and the adduct $(M - 2H + \text{CF}_3\text{COOH})^{2-}$. (The apparent signals greater than m/z 630 in Figure 2a arise from noise that appears at high ring electrode rf amplitudes as the ceramic

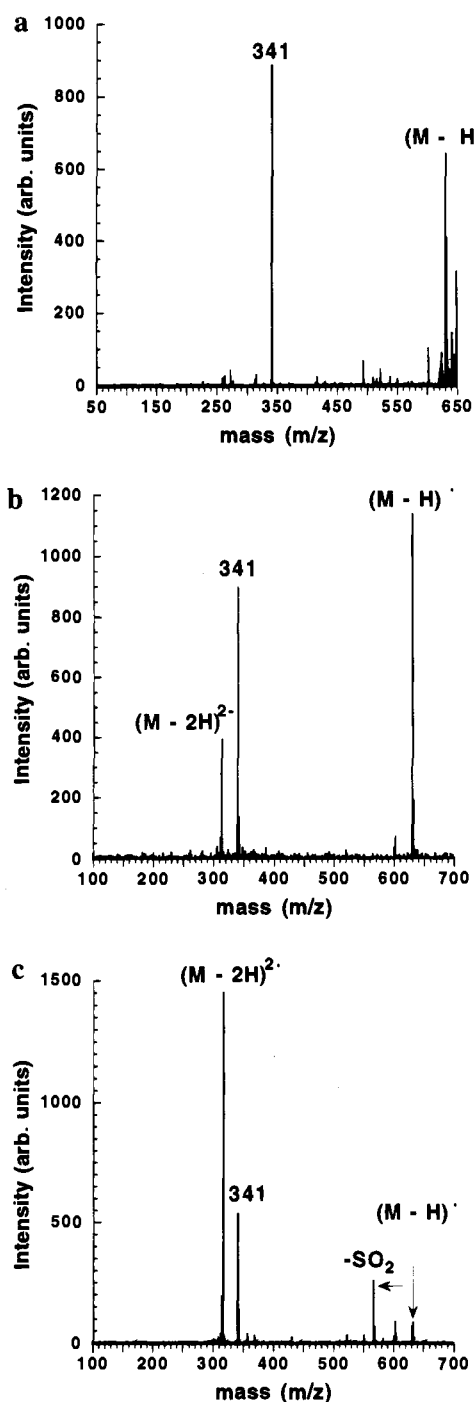
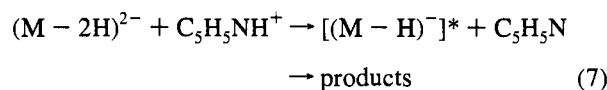


Figure 2. (a) Product ion spectrum resulting from the ion trap collisional activation of $(M - H)^-$ of Direct Red 81 formed by proton transfer from trifluoroacetic acid to $(M - 2H)^{2-}$. (b) The spectrum resulting from the storage of the $(M - 2H)^{2-}$ ion of Direct Red 81 in the presence of protonated pyridine for 200 ms. (c) Ion trap collisional activation of the $(M - 2H)^{2-}$ ion of Direct Red 81 in the presence of ionized xenon for 200 ms.

spacers separating the ion trap electrodes become dirty. This noise is not apparent in the spectra of Figures 2b and 2c because they were acquired using resonance ejection to extend the mass/charge range by a factor of 2 thereby avoiding use of ring electrode rf amplitudes high enough to observe the noise.) Ion trap collisional activation involves multiple low-energy collisions with the background gases, the major component being helium. Ion activation under these conditions is slow and tends

to strongly favor the lowest energy decomposition channels.¹⁶ It is therefore highly likely that the decomposition to yield the product ion at m/z 341 (the fragment to the right of the cleavage indicated in Chart 1) is the lowest energy decomposition pathway for $(M - H)^-$.

Figure 2b shows the products observed from the reaction of $(M - 2H)^{2-}$ with protonated pyridine, i.e.:



In contrast to the results previously reported for the ion/ion proton transfer reactions of multiply-charged oligonucleotide anions with protonated pyridine, some fragmentation of the anion is observed as a result of reaction 7. Clearly, the most abundant fragmentation product appears to coincide with that observed in the spectrum of Figure 2a resulting from ion trap collisional activation of $(M - H)^-$ (see Chart 1). Although some fragmentation is observed, there remains an abundant signal due to $(M - H)^-$ despite the high exothermicity (>100 kcal/mol) expected for such an ion/ion reaction. Figure 2b clearly suggests that more energy is transferred into $(M - H)^-$ upon formation by ion/ion reaction than by ion/molecule reaction. However, the survival of much of the $(M - H)^-$ ion population initially formed by ion/ion proton transfer and the nearly exclusive observation of the decomposition product expected to arise from the lowest energy decomposition channel suggest that much of the reaction exothermicity is partitioned elsewhere and most likely as translational energy of the products.

Figure 2c shows the negative ion spectrum obtained after the $(M - 2H)^{2-}$ ions were allowed to react with singly-charged xenon cations for 200 ms. Ion/molecule proton transfer from adventitious acidic neutrals in the vacuum system, such as carbonic acid, also occurs over this time period and accounts for the observation of $(M - H)^-$. The fragment ions, however, are not observed in the absence of the xenon cations. Electron transfer from $(M - 2H)^{2-}$ to Xe^{+} initially yields $(M - 2H)^{\bullet-}$. However, little or no signal corresponding to this species is observed. Rather, fragment ions appear, some of which are also observed upon collisional activation of $(M - H)^-$ (see Figure 2a) and some of which are not. For example, the formation of the product ion at m/z 341 (see Chart 1) is common to ion/ion electron transfer (Figure 2c), ion/ion proton transfer (Figure 2b), and collisional dissociation of $(M - H)^-$ (Figure 2a). The highly abundant product ion that appears at m/z 565 in Figure 2c, on the other hand, which corresponds to the loss of SO_2 , is essentially absent in the data of Figures 2a and 2b. While it is not surprising that $(M - H)^-$ and $(M - 2H)^{\bullet-}$ share some similar decomposition channels, it is also not surprising that the spectra of their decomposition products can differ significantly. The spectra of Figure 2 clearly demonstrate that ion/ion electron transfer can induce new chemistry, as reflected by the enhancement of SO_2 loss.

The relative absence of the singly-charged radical anion of the azo dye may reflect on either the kinetic stability of the radical anion product, the energy transferred to the anion via the electron transfer process, or both. Unfortunately, $(M - 2H)^{\bullet-}$ product ion stability and internal energy content upon formation cannot be evaluated independently from these data. However, the decomposition behavior of the ion suggests that significant energy randomization occurs in the $(M - 2H)^{\bullet-}$ product ion prior to fragmentation, as reflected by cleavage remote from the initial site of neutralization for the formation of the m/z 341 decomposition product.

5'-d(AAA)-3', 5'-d(AAAA)-3', and 5'-d(AAAAA)-3'. Various charge states of the small oligonucleotides 5'-d(AAA)-3',

(16) (a) March, R. E. *Int. J. Mass Spectrom. Ion Processes* **1992**, *118/119*, 71-135. (b) Todd, J. F. *J. Mass Spectrom. Rev.* **1991**, *10*, 3-52.

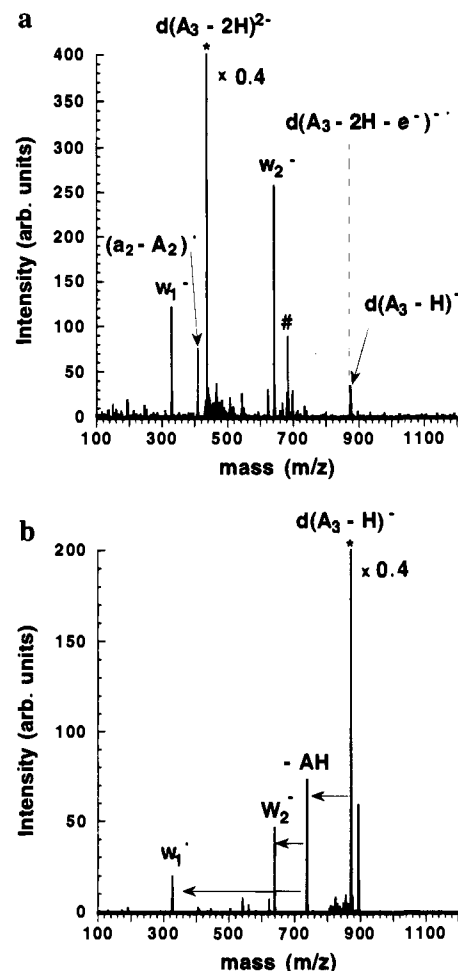
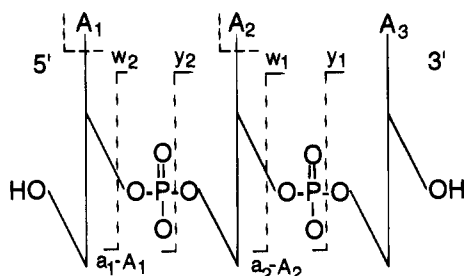


Figure 3. (a) Ion/ion electron transfer spectrum arising from interaction of $d(A_3 - 2H)^{2-}$ with xenon cations for 200 ms. (b) Product ion spectrum resulting from the ion trap collisional activation of $d(A_3 - H)^-$.

Chart 2



$5'-d(AAAA)-3'$, and $5'-d(AAAAA)-3'$ have been subjected to reactions with ionized argon, krypton, and xenon. We have characterized the fragmentation behavior of the even-electron anions of these species,¹⁷ along with a much larger suite of molecules, using ion trap collisional activation. The closed-shell anions of these species fragment by loss of adenine (A) either as an anion or as a neutral,¹⁸ followed by cleavage of the 3' C-O bond of the sugar from which the adenine was lost to yield complementary w-type and (a-A)-type products (see Chart 2). The step-wise formation of these products has been confirmed by multiple stages of ion isolation and collisional activation. These same general tendencies have been observed for a wide variety of small multiply-charged oligonucleotide

(17) McLuckey, S. A.; Vaidyanathan, G. Unpublished Results, Oak Ridge National Laboratory, 1995.

(18) McLuckey, S. A.; Vaidyanathan, G.; Habibi-Goudarzi, S. *J. Mass Spectrom.* **1995**, *30*, 1222-1229.

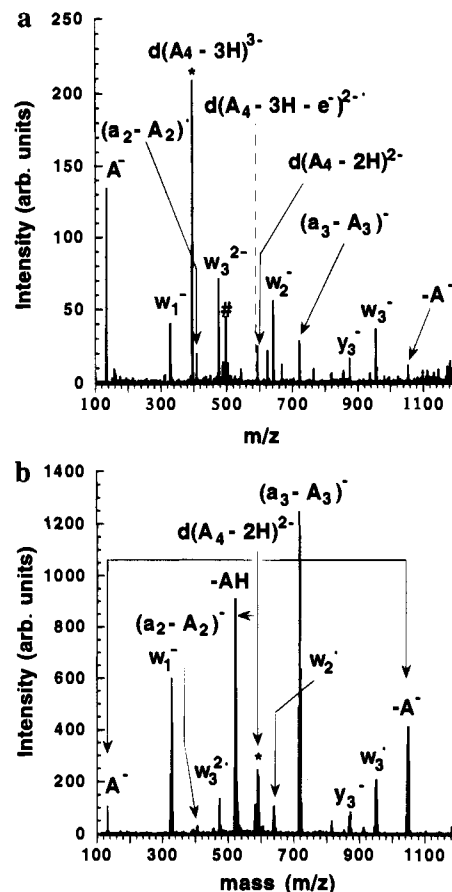


Figure 4. (a) Ion/ion electron transfer spectrum arising from interaction of $d(A_4 - 3H)^{3-}$ with xenon cations for 200 ms. (b) Product ion spectrum resulting from the ion trap collisional activation of $d(A_4 - 2H)^{2-}$.

anions under ion trap collisional activation conditions¹⁹ and by Fourier transform mass spectrometry.²⁰

Figures 3-5 compare spectra resulting from the 200-ms storage of doubly-charged $d(A_3 - 2H)^{2-}$ (Figure 3), triply-charged $d(A_4 - 3H)^{3-}$ (Figure 4), and quadruply-charged $d(A_5 - 4H)^{4-}$ (Figure 5) in the presence of xenon cations with spectra obtained by collisional activation of $d(A_3 - H)^-$, $d(A_4 - 2H)^{2-}$, and $d(A_5 - 3H)^{3-}$, respectively. In all cases, some contribution from ion/molecule proton transfer reactions, arising from the presence of acidic neutrals in the vacuum system, to yield lower charge state even-electron anions is observed. In no case is a significant signal due to an odd-electron electron transfer product anion, such as $d(A_3 - 2H)^{-}$, observed. Rather, a number of fragmentation products are observed that do not appear in the absence of xenon cations. Like the case of the dianion of the azo dye Direct Red 81, ion/ion electron transfer appears to induce fragmentation in essentially 100% of the initially formed $d(A_m - (m - 1)H)^{(m-2)-}$ product anions. (Over 90% of the parent ion loss can be accounted for as fragment ions indicating that ion/ion scattering does not appear to play a significant role in parent ion loss.) Interestingly, most of the fragmentation observed can be rationalized based on the loss of adenine followed by cleavage at the sugar to yield w-type and (a-A)-type products, which generally parallels the behavior of the even-electron ions of the same charge state under ion trap

(19) (a) McLuckey, S. A.; Van Berkel, G. J.; Glish, G. L. *J. Am. Soc. Mass Spectrom.* **1992**, *3*, 60-70. (b) McLuckey, S. A.; Habibi-Goudarzi, S. *J. Am. Chem. Soc.* **1993**, *115*, 12085-12095. (c) McLuckey, S. A.; Habibi-Goudarzi, S. *J. Am. Soc. Mass Spectrom.* **1994**, *5*, 740-747.

(20) Little, D. P.; Chorush, R. A.; Speir, J. P.; Senko, M. W.; Kelleher, N. L.; McLafferty, F. W. *J. Am. Chem. Soc.* **1994**, *116*, 4893-4897.

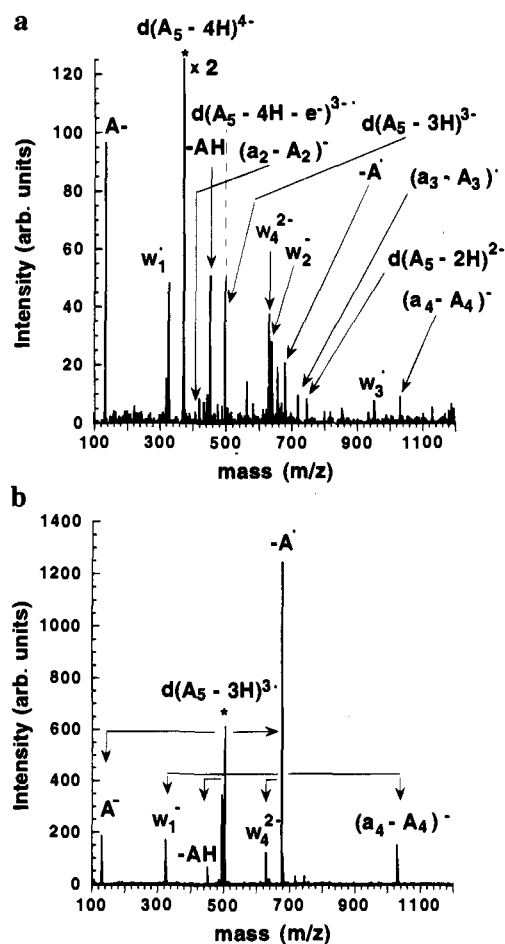
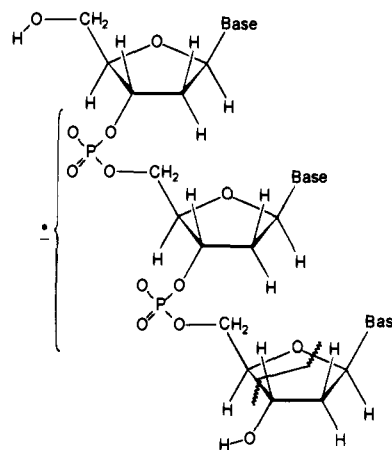


Figure 5. (a) Ion/ion electron transfer spectrum arising from interaction of $d(A_5 - 4H)^{4-}$ with xenon cations for 200 ms. (b) Product ion spectrum resulting from the ion trap collisional activation of $d(A_5 - 3H)^{3-}$.

collisional activation conditions (see Chart 2). However, there are also subtle but significant differences. Each parent ion is discussed in turn below with reference to ion trap collisional activation results derived from the even-electron anion of the same charge state.

Virtually all of the ions in Figure 3a, aside from the $d(A_3 - 2H)^{2-}$ and $d(A_3 - H)^-$ ions, are presumed to arise from fragmentation of $d(A_3 - 2H)^{-}$ formed from ion/ion electron transfer, since they are not observed in the absence of rare-gas cations. The ions labeled as w_1^- , w_2^- , and $(a_2 - A_2)^-$ in Figure 3a are all observed upon ion trap collisional activation of $d(A_3 - H)^-$ (Figure 3b). This suggests that the $d(A_3 - 2H)^{-}$ anion fragments by a similar two-step mechanism in which the base is lost first followed by cleavage at the sugar. While the w-type ions could be formed directly, the $(a_2 - A_2)^-$ anion cannot. A major difference between Figure 3a and Figure 3b, however, is that essentially no signal is observed that corresponds to loss of the base following ion/ion electron transfer whereas loss of a neutral molecule of adenine is the base peak in the collisional activation spectrum. Based on these observations, the observations with Direct Red 81, and the data described below, we surmise that sufficient energy is present in the initially formed $d(A_3 - 2H)^{-}$ anion population to cause both the first step, loss of base, and the second step, cleavage at the sugar, to proceed to completion. However, it is also noteworthy that only minor further fragmentation is observed. That is, the first two steps of the decomposition of the polynucleotide go to completion but relatively little contribution from additional steps is observed. The ion/ion electron transfer data acquired with argon and

Chart 3



krypton ions (not shown) also show a small signal corresponding to deprotonated adenine at m/z 134. In general, the loss of a charged nucleobase competes with the loss of the corresponding neutral^{18,19} in decompositions of oligonucleotide anions. The observation of the A^- loss channel, which is much more prominent for higher charge states (see below), is further evidence for the step-wise decomposition beginning with loss of neutral adenine.

The other major difference between Figure 3a and the collisional activation results for the $(M - H)^-$ ion is that an additional fragment ion, indicated with a # sign in Figure 3a, is observed in the ion/ion electron transfer data which cannot be explained simply by the loss of base and a subsequent fragmentation along the phosphodiester backbone of the oligonucleotide. This fragment ion corresponds to a loss of a terminal base and part of a terminal sugar. A possible mechanism for this decomposition is shown in Chart 3. While other mechanisms could be drawn for this loss, the major point here is that a significant fragmentation channel is present for the radical anion that is essentially absent in the even-electron ion of the same charge state.

Small signals that might arise from the analogous fragmentation can also be assigned in the $d(A_4 - 3H)^{3-}/Xe^{+}$ case but the process is clearly less prominent for the larger and more highly charged oligonucleotides. Otherwise, most of the same overall observations made for $d(A_3 - 2H)^{2-}/Xe^{+}$ apply in interpreting Figures 4 and 5. For example, in the case of $d(A_4 - 3H)^{3-}/Xe^{+}$ (Figure 4), by far most of the fragmentation can be accounted for by base loss followed by cleavage at the 3' C—O bond of the sugar. Loss of adenine as an anion is indicated by the intense signal at m/z 134. The complementary ion, however, is observed in significantly lower abundance. Clearly, further fragmentation occurs leading to much of the other fragment ion signal in the spectrum. A very weak signal is observed that corresponds to the loss of neutral adenine. Further fragmentation of the ion formed by loss of neutral adenine could also account for a significant fraction of the total fragment ion signal. It cannot be determined from these data alone the relative contributions from fragmentation beginning with loss of neutral adenine vs that arising from loss of A^- . (Collisional activation of the $d(A_4 - 2H)^{2-}$ anion (Figure 4b) shows loss of neutral adenine to be more prominent than loss of A^- but both are observed to give rise to significant fragment ion abundances.) However, it is clearly apparent that all of the possible w-type and (a-A)-type fragments are observed in significant abundance from the $d(A_4 - 3H)^{2-}$ anion.

Perhaps the major significant difference between Figure 4a and the collisional activation results from $d(A_4 - 2H)^{2-}$ (Figure

4b) is that formation of the complementary $(a_2 - A_2)^-$ and w_2^- are only minor products in the collisional activation results whereas they are prominent in the ion/ion electron transfer results. The relative lack of contribution due to $(a_2 - A_2)^-$ and w_2^- ions in the collisional activation data from $d(A_4 - 2H)^{2-}$ is attributed to the likelihood that the negative charges tend to reside on the first and third phosphodiester linkages of $d(A_4 - 2H)^{2-}$ to minimize Coulombic repulsion. It has been noted that the presence of a charged phosphodiester linkage on the 3' side of a sugar catalyzes the loss of the base.²¹ The catalytic effect of the charged phosphodiester group and the tendency to minimize Coulombic repulsion would be expected to minimize the formation of $(a_2 - A_2)^-$ and w_2^- ions, as observed in Figure 4b. However, this is not observed from $d(A_4 - 3H)^{2-}$ (Figure 4a). The lack of selectivity with respect to the competition between the various possible base losses from $d(A_4 - 3H)^{2-}$ may arise for energetic or mechanistic reasons, or both. In any case, it may be significant that the factors governing the competition between the various possible base losses and, consequently, the relative contributions from the sequence-specific second generation product ions might differ for radical anions than for even-electron anions.

The data of Figure 5a arising from the $d(A_5 - 4H)^4-/Xe^{+}$ experiment reinforce the observations made regarding the $d(A_4 - 3H)^{3-}/Xe^{+}$ results. Loss of both A^- and neutral adenine are observed along with significant further decomposition yielding w-type and (a-A)-type ions. Signals from all possible channels are observed. Ion trap collisional activation results for $d(A_5 - 3H)^{3-}$ (Figure 5b), on the other hand, show mostly formation of w_4^{2-} and the $w_1^-/(a_4 - A_4)^-$ complementary pair. Formation of the $w_2^-/(a_3 - A_3)^-$ pair is a very minor process and the $w_3^-/(a_2 - A_2)^-$ pair is essentially absent. The $(a_2 - A_2)^-$ ion is also quite small in Figure 5a but is more prominent in the $d(A_5 - 4H)^4-/Ar^{+}$ and $d(A_5 - 4H)^4-/Kr^{+}$ results discussed below (see Figure 6). As with all of the other ion/ion electron transfer data presented here involving multiply-charged oligonucleotide anions, little or no primary reaction product, $d(A_5 - 4H)^{3-}$, is observed. As the size of the oligonucleotide increases, the abundance of the product ions formed by base loss increases but significant further decomposition to yield sequence informative fragmentation is also observed.

Data for all three of the oligonucleotide anions were also acquired with Ar^{+} and Kr^{+} as the cationic reactants. Figure 6 shows the results for (a) $d(A_5 - 4H)^4-/Ar^{+}$ and (b) $d(A_5 - 4H)^4-/Kr^{+}$ (see also Figure 5a for $d(A_5 - 4H)^4-/Xe^{+}$ data). The overall exothermicity of the reactions increases in the order xenon (IP = 12.1 eV), krypton (IP = 14 eV), argon (IP = 15.8 eV).²² However, significant differences in the extent of fragmentation between the various cations for a given anion are not observed. In all cases, the reactions are expected to be highly exothermic. Although the electron affinities of the ion/ion electron transfer products are not known quantitatively, they are likely to be small in magnitude (<1 eV) and possibly even negative in sign.²³ Therefore, the reactions are expected to be at least 11 eV (>250 kcal/mol) exothermic. The relative

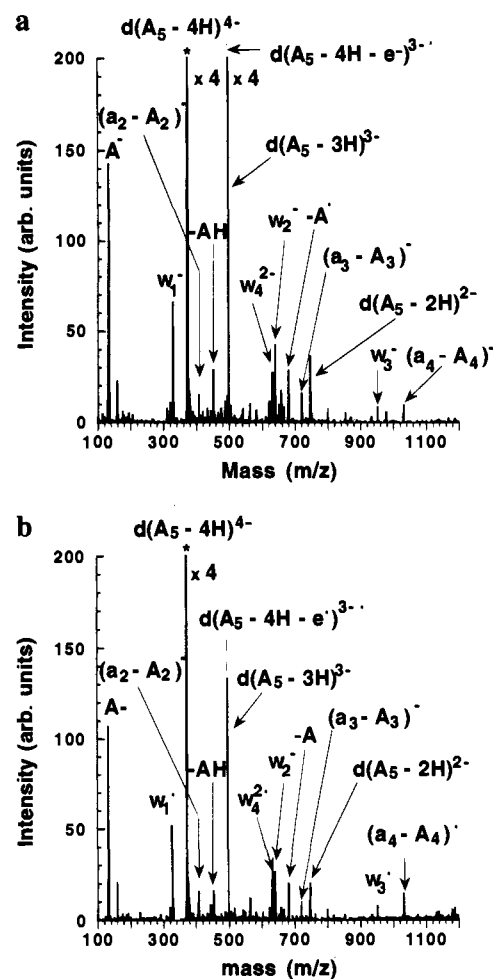


Figure 6. (a) Ion/ion electron transfer spectrum arising from interaction of $d(A_5 - 4H)^4-$ with argon cations for 200 ms. (b) Ion/ion electron transfer spectrum arising from interaction of $d(A_5 - 4H)^4-$ with krypton cations for 200 ms.

insensitivity of the ion/ion electron transfer spectra to the ionization potential of the rare gases over the IP range studied here (2.7 eV) is therefore not particularly surprising given both that 2.7 eV is a relatively small fraction of the greater than 11 eV reaction exothermicity and that much of the reaction exothermicity can be partitioned into product ion translation.

Rate constant measurements for ion/ion electron transfer reactions were not made in this work due to complications arising from the rapid loss of rare gas cations due to charge transfer with background gases, such as oxygen and water vapor. However, these reactions are expected to be essentially unit efficient, due to their high exothermicity, and should therefore proceed at the ion/ion collision rate. The rate constants for these reactions are therefore expected to be similar to those measured for ion/ion proton transfer reactions⁸. It has already been noted that reaction rates are maximized in the Paul trap when anion and cation spatial overlap is maximized. It is therefore desirable to minimize the difference in mass-to-charge ratio of the reactants and to store them at the greatest well-depths possible. In this regard, of the rare gas cations used in this study, xenon cations are most useful. Xenon allows all reactant ions to be stored at higher well-depths than can argon or krypton, which is also desirable for storing the high mass-to-charge fragment ions formed from the reactions. Furthermore, xenon cations are depleted less quickly via charge transfer with background gases.

(21) (a) Cerny, R. L.; Gross, M. L.; Grotjahn, L. *Anal. Biochem.* **1986**, *156*, 424–435. (b) Phillips, D. R.; McCloskey, J. A. *Int. J. Mass Spectrom. Ion Processes* **1993**, *128*, 61–82. (c) Rodgers, M. T.; Campbell, S.; Marzluff, E. M.; Beauchamp, J. L. *Int. J. Mass Spectrom. Ion Processes* **1994**, *137*, 121–149. (d) Habibi-Goudarzi, S.; McLuckey, S. A. *J. Am. Soc. Mass Spectrom.* **1995**, *6*, 102–113.

(22) Lias, S. G.; Bartmess, J. E.; Liebman, J. F.; Holmes, J. L.; Levin, R. D.; Mallard, W. G. *J. Phys. Chem. Ref. Data* **1988**, *17*, Suppl. 1.

(23) Even slightly negative values for electron affinities for multiply-charged anions can still lead to stable dianions due to the Coulombic barrier in the exit channel on charge separation. See, for example, ref 9d.

Conclusions

Multiply-charged high-mass anions engage in highly exothermic electron transfer reactions with rare gas cations in the gas phase. Essentially all of the odd-electron product anions formed by this reaction in this work dissociate via relatively low energy decomposition channels. In the case of polyadenylate anions, most product ions fragment by base loss followed by cleavage at the sugar from which the base was lost, in analogy with even-electron anions of the same charge state. However, odd-electron anions were also observed to show fragmentation pathways not observed from the analogous even-electron anions. Furthermore, ion/ion electron transfer reactions involving polyadenylate anions show contributions from all of the major competitive decomposition channels, whereas fewer channels are observed upon ion trap collisional activation of the analogous closed-shell anions.

Ion/ion proton transfer reactions lead to little or no fragmentation of the product ions under otherwise identical conditions. The efficient fragmentation observed for ion/ion electron transfer reactions could be related to limited kinetic stability of the radical anion product, the greater reaction exothermicity associated with the electron transfer reactions studied here relative to the ion/ion proton transfer reactions, a greater fraction of

reaction exothermicity partitioned into product anion internal energy, or a combination of these factors. Differences in the fragmentation behavior observed for the even- and odd-electron anions of the same charge state could arise from mechanistic, structural, and energetic origins. The fact that the radical anion presumed to be formed initially upon electron transfer was not observed in the time frame of these experiments made difficult a separation of structural/mechanistic contributions to the observed fragmentation patterns from contributions from the reaction energetics. Nevertheless, it is clear that ion/ion electron transfer reactions involving high-mass multiply-charged anions to yield odd-electron species can lead to behavior not observed from even-electron species. New information might therefore be gained that is largely complementary to that obtained by other methods used to probe high-mass ions.

Acknowledgment. W.J.H. acknowledges support through an appointment to the Oak Ridge National Laboratory Postdoctoral Research Associates Program administered jointly by the Oak Ridge Institute for Science and Education and Oak Ridge National Laboratory. This work was supported by the National Institutes of Health under Grant No. R01GM45372.

JA9520171